# Risk assessment of electrofusion joints in commissioning of polyethylene natural gas networks

Abolfazl Tutunchi[a], Mehdi Eskandarzade[b*], Reza Aghamohammadi[a], TaherehMasalehdan[a], Karim Osouli-Bostanabad[a]

[a] Department of Materials Engineering, Institute of Mechanical Engineering, University of Tabriz, Tabriz, 51666-16444, Iran

[b] Department of Mechanical Engineering, University of Mohaghegh Ardabili, Ardabil, P.C.: 5661745711, Iran

* Corresponding author: E-mail address: m.eskandarzade@gmail.com (M. Eskandarzade).

**Abstract**

The application of polyethylene pipes and equipment in the natural gas networks is continuously increasing due to their competitive weight and cost compared to metallic materials. Electrofusion welding is an effective and fast approach for the production of polyethylene joints with high safety and endurance. However, recently intermittent failures have reported in underground polyethylene piping networks. Although the failure frequencies are low, but disasters could happen due to the failure in gas pipelines as they usually buried in populated areas. In this study a combination of Failure Mode and Effects Analysis (FMEA), and empirical methods were used to identify main damage mechanisms incorporated to intermittent failures of polyethylene natural gas networks. After performing the FMEA process, based on the obtained risk ranking, three most critical damage mechanisms, including improper scraping, lipid contaminations, and humidity existence in weld zones were investigated experimentally to determine their practical severity. According to empirical evaluations, improper scraping was the most severe damage mechanism, followed by the contaminated welding surfaces during the weld construction.

**Keywords**: Electrofusion welding, Natural gas network, FMEA, Polyethylene

**Abbreviations**

FMEA: Failure Mode and Effects Analysis

PEPs: Polyethylene pipes

NDE: Non-destructive evaluation

POF: Probability of Failure

COF: Consequence of Failure

PFDs: Piping flow diagrams

P&I: Dinstrumentation diagrams

SEM: Scanning electron microscope

CT-scans: Computerized tomography scans

## 1. Introduction

Polyethylene pipes (PEPs) for natural gas network applications have first been used in the USA in the late 1950s and got interested in Europe after 1970s [1]. PEPs and equipment used in gas networks are cost-effective, non-toxic, resistant to corrosion and have increased life cycle (about 100 years) [2]. In a study by Bachir-Bey et al. [3], some portions of PEPs were cut after almost 30 years of operation and no sign of aging in terms of mechanical properties were observed. However, intermittent failures in this type of piping networks have been reported in different countries. The failures statistical data of a natural gas network in the USA between 2004 and 2015 were investigated by Bianchini et al. [4] indicating frequency of accidents of about

failures per kilometer per a year. Additionally, they found that the average number of injuries and fatalities in low-pressure small diameter natural gas systems is even higher than high-pressure-large diameter piping networks.

The most critical threat to the integrity of polyethylene piping systems is a leakage from electrofusion joints. In contrary to steel pipes, non-destructive evaluation (NDE) of PEPs is a challenging task. Recently, researchers attempted to employ a combination of artificial intelligence and traditional NDE methods to determine defects in electrofusion joints [5,6]. In addition to NDE limitations, the main problem in the design of electrofusion joints is lack of comprehensive knowledge on PEPs physicochemical characteristics that affect their mechanical behavior and performances. For instance a crack growth as one of these challenging issues is under investigation by several researchers [7,8]. Recent reports showed that the failures normally occur due to micro-cracks initiation at the interface of a pipe and coupler, where subsequent growth of micro-cracks leads to a brittle fracture [7,8].

It has been reported that the main reason for most of failures in electrofusion joints could be related to application of low-quality materials and non-standard construction procedures [9]. The source of many defects in electrofusion joints is related to the weld surface preparation step and other pre-welding activities during the construction phase. Towards, welders qualification is a crucial factor in achieving high quality joints [10]. The strength of electrofusion joints depends on the welding temperature, dwell time for heating and cooling, cleanliness of the parent surfaces, and the pipe and coupler alignment [11]. The cleanliness of the parent surfaces is a vital parameter and even a small pollutant on the welding surfaces can substantially reduce the joint-life [12]. The scraping of the parent surfaces before the welding not only removes all contaminations from the surfaces, but also removes all oxide layers from the welding region [13]. The oxide layers on the surface of

PEPs prevent homogeneous mix-ability of the pipe and coupler melts through the welding process [14]. Therefore, scraping of the pipe surface before the welding process is an essential step to ensure that the contaminations such as pollutants, greases, humidity, and dusts are completely removed from the welding region [15]. To achieve satisfactory welded joints, the welding temperature also needs to be set in a range of technically confirmed high-working-temperature. Researches have shown that the melt pressure at the welding cavity is too low to fill all gaps between the coupler and pipe when welding in low-temperature regimes [16]. Therefore, weather condition at the time of welding is very important in electrofusion welding process [17]. Recently, Ramadan and Tanase [18] studied the influence of welding parameters on structural integrity of PEPs and concluded that rapid cooling of the welding zone due to a cold weather can be one of the main sources of intermittent failures in PEP pipelines. The effect of pre-heating in the quality of electrofusion joints is investigated by Najafigharehtapeh and Kaçar [19].

Tutunchi et al. [20] ranked the possible failure mechanisms in the commissioning stage of the urban natural gas systems and determined the most critical locations for monitoring and inspection priority purposes. Review of literatures showed that most of failure modes and imperfection types in PEPs have been presented and studied by many researchers [21,22] However, to the best knowledge of authors there is no risk ranking of imperfections in literatures. This study employed the risk assessment concept to identify root causes of intermittent failures in polyethylene natural gas piping systems. This risk assessment procedure begins with FMEA, which determines the three most critical failure mechanisms in PEPs and continue with empirical analyses, which ranks the highlighted mechanisms based on their severity. Fig. 1 shows the process followed in this work.

**Fig. 1**

## 2. Process and methodology

### *2.1. FMEA technique*

FMEA is a systematic way of recognizing a failure mechanism in materials and processes [18]. It has many applications in the oil and gas industries. Fig. 2 shows different steps of the FMEA. It includes the following steps:

1- Process definition: the main goal of this stage is to define the scope of the assessment procedure. It helps to break the whole process down into different phases to make the events manageable. A team of engineers, with various disciplines, including manufacturing, construction, commissioning, and integrity typically are taking part in this step.

**Fig. 2**

2- Failure mode analysis: in this step, all parameters related to the process (e.g. welding temperature, the pipe surface preparation, and etc), operation, construction, and procurement steps, and also the associated damage mechanisms were determined and classified.

3- Probability of Failure (POF) and Consequence of Failure (COF) estimations: in this step, considering the general failure frequencies in the industry and taking into account the failure history of the component, the PoF and CoF scores for each active damage mechanism were calculated.

4- Risk identification: in this step, the POF and COF scores for each damage mechanism were combined to calculate the failure risk of the component. Subsequently, damage mechanisms were ranked based on their severity (Fig. 3).

5- Damage mitigation strategies: based on identified risk categories for each damage mechanism, mitigation techniques such as inspection methods, inspection intervals, and replacement strategies were suggested. The goal of this step was decreasing the failure risk of each active damage mechanism to an amount lower than the target risk level.

**Fig. 3**

A natural gas pipeline network of residential and industrial areas of Urmia, Iran (a 5543 km underground piping system) is made of PEPs mostly in diameters of 90 mm, 63 mm, and 25 mm. The operating pressure of this network is about 0.4 MPa. The highest failure rate has been reported in piping systems with diameters of 25 mm and 63 mm (i.e. $1.3\times10^{-3}$ failure per kilometer per a year).

A risk assessment process was used to identify failure sources, to manage and control the rate of accidents in this network. In this regards, a team of experienced engineers was employed to implement FMEA technique and to determine active damage mechanisms in a polyethylene natural gas piping network of Urmia. Related documents, including piping flow diagrams (PFDs), piping and instrumentation diagrams (P&ID), inspection histories, anomaly record, and other repair and maintenance documents were provided prior the brainstorm session for the team members from departments of inspection, maintenance, construction, health and safety. At the session time, besides the twenty years' anomaly report of the Urmia natural gas company, it was asked from each team member to mention own knowledge and experiences regarding active damage mechanisms in each stage of the network lifecycle, individually. Based on the risk ranking of the damage mechanisms, three most critical mechanisms were selected for further experimental evaluations.

The risk assessment team members were asked to determine POF and COF scores for each damage mechanism using tables prepared based on improved Kent Muhlbauer formula (Eq. (1)). In Eq. (1) $M$ and $S$ indicate coefficients for the mitigation and survivability parameters, respectively. Furthermore, $w_m$ and $w_s$ are weight factors which balance the effects of the mitigation and survivability parameters, respectively. In this study, both these parameters were set to be 0.5; means equal effect of mitigation and survivability factors. In addition, in Eq. (1) the unit of is failure per year per kilometer and represents a generic POF value of the damage mechanism and equals the failure frequency due to that specific damage type based on historical failure records. Table 1 shows generic POFs for different damage mechanisms based on twenty years' failure reports of the Urmia natural gas pipeline.

$$\text{POF} = a \times (1-w_m .M) \times (1- w_s.S) \quad (1)$$

Table 1. Generic POFs (a) for different damage types.

| Damage type | Generic POFs (a) |
|---|---|
| Physical damage | $1.01 \times 10^{-2}$ |
| Poor procurement | $1.04 \times 10^{-4}$ |
| Humidity at the welding surfaces | $1.01 \times 10^{-2}$ |
| Improper scrapping | $1.2 \times 10^{-2}$ |
| Lipid type pollutants | $1.02 \times 10^{-2}$ |
| Misalignment of the joints | $1.03 \times 10^{-3}$ |
| Unsuitable welding temperature | $1.03 \times 10^{-5}$ |
| Equipment failure | $1.05 \times 10^{-4}$ |
| Shaking and mechanical damages | $1.01 \times 10^{-4}$ |
| Nonstandard maintenance | $1.00 \times 10^{-3}$ |

Mitigation coefficient (M) reflects the effect of the type and effectiveness of every mitigation measure designed to block or reduce an exposer. A subject matter engineer compared the ideal mitigation measures with available mitigation measures at the system and estimated the mitigation coefficient (M) for damage types. On the other hand, survivability (S) is the inherent ability of a piping material to sustain forces and deformations in the event of mitigation failure. The construction materials and fabrication quality dictates the value of the S parameter. The risk assessment team listed all potential abilities of the used material to sustain against each exposer. The appraisal decided how much percent of the ideal survivability has been satisfied in current piping system. In order to reduce the effect of human bias and avoid the influence of artificial preferences the average coefficient determined by three or more experts, as per Eq. (2), was used for POF and COF calculations.

$$M = \frac{\sum_{i=1}^{n} m_i}{n} \qquad (2)$$

where, n is the number of appraisers, and $m_i$ is the mitigation coefficient estimation of appraiser number i. After determination of POFs and COFs, the risk level of damage mechanisms were determined. In this study risk matrix as Fig. 3 was used to combine POFs and COFs.

***2.2. Experimental methodology***

In the empirical part of this study, polyethylene pipes (grade of PE-100-SDR11) with outer diameter of 63 mm in lengths of 500 mm were supplied by local vendors in sufficient numbers. The required numbers of couplers were supplied by the same company. Before the welding, samples were scraped using a scraper in accordance with the written procedure, then samples were cleaned using acetone solution (98%) and a piece of fabric. The equipment specifications of used technique were satisfied the requirements of the electrofusion welding procedure and the requirements specified by the material vendor.

In order to investigate the effects of various defects in the final joint quality, several artificial defects at the welding zones were created. To preserve data validity and experiments repeatability, an aluminum foil as stencil was used according to Fig. 4(a) to artifact aimed defects. However, defects in type of "non-scraped regions" were fabricated using the method presented in Fig. 4(b). Samples with properly scrapped surfaces using a standard scraping device were also prepared and used as the control group.

**Fig. 4**

Three types of artificial defects in three different sizes, including improper scraping, lipid pollutants, and moistures in weld zones were created based on the aforementioned procedure. Fig. 5 shows two examples of the prepared defective samples. Indeed, three types of damages, each in three sizes, were investigated. In order to check the repeatability of the results each test was repeated two times. Therefore, in total 27 electrofusion joints were analyzed. Three sizes of artifact defects were 15 mm × 15 mm, 25 mm × 15 mm, and 35 mm × 15 mm. It means all samples with lipids, liquid moistures, and improper-scraping had defects with three sizes at welding surfaces of their pipes before the alignment of the pipe and coupler. Glycerin was used as a lipid pollutant in welding areas. The welding time was set automatically by the welding equipment based on the manufacturer datasheets.

**Fig. 5**

Table 2 indicates heating and cooling time laps of the welding coils. Fig. 6 shows the setup was used in empirical assessments throughout the current study. A crushing de-cohesion test was performed on electrofusion joints containing fabricated defects. The tests were conducted based on the requirements specified in the ISO-13955 standard. According to the engineering best practices, any joint with brittle fracture surface lower than 20% under the crushing de-cohesion test was considered acceptable. Before performing the crushing de-cohesion tests, polyethylene joints were cut alongside the longitudinal axis into two parts, and their interfaces were inspected visually for the presence of any defects.

Table 2. Electrofusion welding parameters.

| Coupler | Heating time of coupler elements | Initial cooling time | Total cooling time | Welding voltage |
|---|---|---|---|---|
| Sample no. 1 | 93 s | 12 min | 30 min | 38 V |

**Fig. 6**

In addition, the strip-bend test was used to estimate the amount of parent materials fusion. The strip-bend test is an accurate and sensitive test reflecting the severity of defects in electrofusion joints. According to engineering best practices, a fracture surface of a perfect weld consists only 20% or lower area with brittle fracture evidences after the strip-bend test. In the present study the fracture surfaces of the strip-bend tests were examined using an optical microscope and a scanning electron microscope (SEM).

**3. Results and discussion**

### *3.1. FMEA analysis*

Table 3 shows the result of FMEA analyses for the damage mechanism identification. Also Table 4 shows the result of mitigation analyses for this piping network. Through Table 4 the appraisal team compared the ideal mitigation actions with available mitigation actions for the PE piping network of present study and the average of their assigned scores is presented as average mitigation coefficient (*M*) in Table 4. Similar comparisons made for survivability and results are provided in Table 5.

Table 3. Identification of damage mechanisms- FMEA analysis.

| No. | Executive Phase | Failure mechanism | Risk Driver |
|---|---|---|---|
| 1 | Loading and transportation | Physical damage | Unsuitable loading |
| | | Poor procurement | Welding using pipe and coupler from different brands |
| 2 | Construction | Humidity at the welding surfaces | Weather condition or other humidity sources |
| | | Improper scrapping | Scrapping using non-standard devices<br>Improper scrapping<br>Long waiting time between scrapping and welding |
| | | Lipid type pollutants | Unsuitable solution |
| | | Misalignment of the joints | Using non-standard alignment devices |
| | | Other pollutants | Using unsuitable fabric |
| | | Unsuitable welding temperature | Not following standard procedures |
| | | Unsuitable Cooling and warming time | Not following standard procedures<br>Insufficient cooling time<br>Excess welding time |
| | | Welding equipment fault | Unsuitable voltage<br>Unsuitable welding time<br>Defective coupler switches |
| | | Lack of complete coupling between electrical socket and coupler switch | Using not calibrated welding device<br>Lack of control on output voltage |
| 3 | Operation | Shaking and mechanical damages | Lack of protective measures |
| | | Cyclic loads especially for small bore branches | Harsh operating condition |
| | | Nonstandard maintenance | Not following the written procedures |

Table 4. Ideal mitigation measures versus average mitigation coefficient (*M*) for the current case study.

| Damage mechanism | Mitigation 1 | Mitigation 2 | Mitigation 3 | Average mitigation coefficient (*M*) |
|---|---|---|---|---|
| Physical damage | Control on loading | Control on unloading | – | 50% |
| Poor procurement | Qualified purchase order | Vendor reputation | Shop inspection | 70% |
| Humidity at the welding surfaces | Check welding surfaces | Check weather condition | – | 20% |
| Improper scrapping | Check devices | Establish scrapping procedure | Random checks by inspection engineer | 40% |
| Lipid type pollutants | Check cleaner type | Check for pollutant sources | Use clean and non-fluffy fabric for clean the welding surfaces | 80% |
| Misalignment of the joints | Check alignment devices | Control excavation condition | – | 90% |
| Unsuitable welding temperature | Check weather condition | Use pre-heat and post heats | Use tent | 20% |
| Equipment failure | Follow component data sheet | Check welding voltage | Check welding time | 20% |
| Shaking and mechanical damages | Use alarm signs and protective measures in welding area | Use protective measures | Take care of cyclic load on new joints | 90% |
| Nonstandard maintenance | Maintenance procedure | Quality control | Pressure test | 100% |

Table 5. Possible survivability options versus survivability coefficient (*S*) of case study.

| Damage mechanism | Survivability 1 | Survivability 2 | Average survivability coefficient (*S*) |
|---|---|---|---|
| Physical damage | Polyethylene Structural integrity | Pipe diameter | 0.8 |
| Poor procurement | – | – | 0 |
| Humidity at the welding surfaces | Weldability of the material under humidity | Welding voltage | 0.2 |

| | | | |
|---|---|---|---|
| Improper scrapping | PE grade fusion capability | | 0.2 |
| Lipid type pollutants | – | – | 0 |
| Misalignment of the joints | Misalignment quality and range | | 0.5 |
| Unsuitable welding temperature | – | – | 0 |
| Equipment failure | – | – | 0 |
| Shaking and mechanical damages | Stress concentration factor of the material grade | Number of hours working under cyclic loads | 0.4 |
| Nonstandard maintenance | – | – | 0 |

Table 6 summaries the risk parameters of the present piping network. The categorization of POFs into five levels from 1 to 5 was done based on Table 7. From Table 6 it can be concluded that three damage mechanisms, including (i) humidity at the welding surfaces, (ii) improper scrapping, and (iii) lipid type pollutants have POF score of 4 and therefore have the highest probability of occurrence. In next steps the COFs were estimated for different damage mechanisms.

Table 6. Summary of the risk parameters of PEP damage mechanisms for the case study.

| **Damage mechanism** | ***A*** | ***M*** | ***S*** | $w_m$ | $w_s$ | **POF** | **POF category** |
|---|---|---|---|---|---|---|---|
| Physical damage | $1.01 \times 10^{-3}$ | 50% | 0.8 | 0.5 | 0.5 | 4.55e-04 | 3 |
| Poor procurement | $1.04 \times 10^{-4}$ | 70% | 0 | 0.5 | 0.5 | 6.76e-05 | 2 |
| Humidity at the welding surfaces | $1.01 \times 10^{-2}$ | 20% | 0.2 | 0.5 | 0.5 | 8.18e-03 | 4 |
| Improper scrapping | $1.2 \times 10^{-2}$ | 40% | 0.2 | 0.5 | 0.5 | 7.34e-03 | 4 |
| Lipid type pollutants | $1.02 \times 10^{-2}$ | 80% | 0 | 0.5 | 0.5 | 6.12e-03 | 4 |
| Misalignment of the joints | $1.03 \times 10^{-4}$ | 90% | 0.5 | 0.5 | 0.5 | 4.25e-05 | 2 |
| Unsuitable welding temperature | $1.03 \times 10^{-5}$ | 20% | 0 | 0.5 | 0.5 | 9.27e-06 | 1 |
| Equipment failure | $1.05 \times 10^{-4}$ | 20% | 0 | 0.5 | 0.5 | 9.45e-05 | 2 |
| Shaking and mechanical damages | $1.01 \times 10^{-4}$ | 90% | 0.4 | 0.5 | 0.5 | 4.44e-05 | 2 |
| Nonstandard maintenance | $1.00 \times 10^{-4}$ | 100% | 0 | 0.5 | 0.5 | 5.00e-05 | 2 |

Table 7. Five levels of POF.

| | **POF value** | **POF category** |
|---|---|---|
| **Highly unlikely** | $9.9 \times 10^{-6} > \text{POF}$ | 1 |
| **unlikely** | $9.9 \times 10^{-6} < \text{POF} < 9.9 \times 10^{-5}$ | 2 |
| **Possible** | $9.9 \times 10^{-5} < \text{POF} < 9.9 \times 10^{-4}$ | 3 |
| **Likely** | $9.9 \times 10^{-4} < \text{POF} < 9.9 \times 10^{-3}$ | 4 |
| **Very likely** | $\text{POF} < 9.9 \times 10^{-3}$ | 5 |

As the fluid type, explosion and ignition probability were the same for all damage types, in estimation of COFs for damage types the time and location of the events were considered. Some of imperfections may result in a failure at the joint site in a pressure test and during the construction stage. Therefore, they could be detected in the construction or pre-commissioning phase by doing these investigations. However, some other damage mechanisms may have delayed effects (i.e. not showing a failure during the construction or in the initial operation period) and reduce the strength of the joint without immediate leakage. These last scenario is the worst case and generally its consequences are much dangerous. Consequently, different damage types may have different consequences based on their detection stage in a piping network lifecycle [[23], [24], [25]]. Given the detection phase of the project, each damage type is categorized as A to E consequence levels with E is the highest consequence value. Using Fig. 3 to combine the achieved POF and COF, the risk category of each damage mechanism was obtained and presented in Table 8. As they are shown in italic format in Table 8, three damage types, including humidity at the welding surfaces, improper scrapping, and lipid type pollutants were the most critical damage types with highest risk level (Medium to High). These damage types are selected for further experimental study in next steps.

Table 8. Result of the risk assessment for PE piping network of the present study.

| **Damage mechanism** | **POF** | **Detection phase of the project** | **COF** | **Risk level** |
|---|---|---|---|---|
| Physical damage | 3 | Pressure test | B | Low |
| Poor procurement | 2 | Pressure test | B | Low |
| *Humidity at the welding surfaces* | *4* | *Operation* | *D* | *Medium High* |
| *Improper scrapping* | *4* | *Operation* | *D* | *Medium High* |
| *Lipid type pollutants* | *4* | *Operation* | *D* | *Medium High* |
| Misalignment of the joints | 2 | Operation | D | Medium |
| Unsuitable welding temperature | 1 | Pressure test | B | Low |
| Equipment failure | 2 | Pressure test | B | Low |
| Shaking and mechanical damages | 2 | Operation | D | Medium |
| Nonstandard maintenance | 2 | Operation | D | Medium |

### *3.2. Experimental analysis*

Fig. 7 shows CT-scans of samples containing man-made defects. The CT-scan was used to trace the fabricated defects at welding areas.

**Fig. 7**

Fig. 8 shows the crushing de-cohesion tests of this study. The crushing de-cohesion tests were performed on electrofusion joints containing man-made defects. Experimental data revealed that test results for all samples, including both appropriately welded and manipulated joints, fall in acceptable ranges in accordance with the Urmia Natural Gas Company's procedure. It can be concluded that these kinds of tests are not sensitive enough to recognize a defective joint from a non-defective joints. Consequently, it was not suitable for the goal of this research and therefore, decided not to continue with this type of tests.

**Fig. 8**

In contrary the strip-bend test has enough sensitivity to discriminate defective joints from appropriately welded joints and used to assess the severity of damage mechanisms in samples. Fig. 9 shows the fractured interface of a sample after the strip-bend test. As it is clear from Fig. 9, some parts of the fractured surfaces are rough, which shows the sign of plastic deformation and is a characteristic of a proper joint and a ductile fracture [[26], [27], [28]]. Additionally, some other parts of the fractured surfaces show smooth areas without any evidence of plastic deformations, which are the characteristics of a brittle fracture [[29], [30], [31]]. Fig. 10 shows the macro-graphs of the fractured surfaces at the defective regions. The fractured surface of the sample with improper scraping (Fig. 10 a) shows an obvious boundary between the scrapped and un-scrapped regions. The scrapped region contains a sign of plastic deformations representative of a well adhesion between the pipe and coupler; however, no signs of plastic deformations observed in the un-scrapped region, implying that the fracture type was brittle and a weak adhesion between the pipe and coupler was occurred. In Fig. 10 (b and c) most areas show evidence of ductile fractures and plastic deformations before the fracture. It means that humidity and lipid type pollutants were not impacted the quality of electrofusion joints, significantly. The fracture surfaces of samples containing humidity and lipid type pollutants for detailed and more accurate investigations were studied using an SEM.

**Fig. 9**

Overall, the fracture surface of samples showed partially characteristics of both the ductile and brittle fractures in different fractions for three studied defect types. Fig. 11 shows the brittle fracture areas of samples related to lipid and moisture pollutants. A fully brittle fracture is obvious from the fractured surface of the sample for lipid type pollutant, while a better adhesion between the pipe and coupler could be concluded from the type of ductile fracture of the sample with trapped moistures.

**Fig. 10**

Table 9 summaries the percentages of brittle and ductile fractures for different samples. It can be seen that the proper scraping is more critical for the integrity of the electrofusion joints. For improper scraping, the area percentage of the brittle fracture for all defect sizes were higher than 20%, so considered as unacceptable preparation. Therefore, even leaving a small area without scraping during the electrofusion welding could considerably reduce the strength of the joint. Although, the results of the strip-bend test fall within an acceptable range for all samples with humidity and lipid type defects. The brittle fracture percentages for lipid type pollutants were higher than those of humidity type pollutants.

**Fig. 11**

Table 9. Brittle fracture percentage ($L_d$) in samples with different defect types and sizes.

| Defect type | Defect size | ($L_d$) % | result |
|---|---|---|---|
| Sound joint | – | | The joint is sound and without any defect. Test results are acceptable |
| Improper scraping | small | 20 | Strip-bend test is sensitive to this type of defect and share of the brittle fracture increases by increasing the defect size. |
| | medium | 27 | |
| | large | 32 | |
| Humidity in the weld zone | small | 10 | Strip-bend test results for all humidity content samples fall within acceptable range |
| | medium | 14 | |
| | large | 18 | |
| Lipid type pollution in the weld zone | small | 15 | Although that all joints with lipid type defects passed the standard criteria, the brittle fracture percentages were considerable. |
| | medium | 18 | |
| | large | 19 | |

## 4. Conclusion

In this study, FMEA was conducted to identify the root cause of failures in polyethylene natural gas networks of a city in Iran. According to the results, three damage mechanisms in polyethylene networks, including (1) improper scraping, (2) trapped moistures, and (3) incorporation of lipid type pollutants in a welding zone were identified as the most critical failure mechanisms. Empirical assessments were performed to study the severity and share of these damages in welds failure during operation period. The most critical damage mechanism was found to be improper scraping, which followed by lipid type pollutants in the weld zone. The results indicated that, defects caused from trapped moistures in the welding zone compared to other two defects had fewer impacts on the quality of electrofusion joints. This could not be traced using crushing de-cohesion but with strip-bend tests. It is suggested to use stricter quality control measures for the scraping stage of the electrofusion welding to prevent and reduce the number of intermittent failures during the operation period in polyethylene joints.

## Author statement

Abolfazl Tutunchi: Conceptualization, Methodology, Mehdi Eskandarzade: Data curation, Writing – original draft preparation Reza Aghamohammadi: Software, Validation Tahereh Masalehdan: Data curation, Visualization Karim Osouli-Bostanabad: Writing – original draft preparation.

## Declaration of competing interest

The authors declare that they have no known competing financial interests or personal relationships that could have appeared to influence the work reported in this paper.

## References

[1] L.L. Bohm, H.F. Enderle, M. Fleifßner High-density polyethylene pipe resins Adv. Mater., 4 (3) (1992), pp. 234-238

[2] C. O'Connor The nature of polyethylene pipe failure Modern Plastic. Worldwide, 88 (2) (2011), pp. 20-22

[3] T. Bachir-Bey, N. Belhaneche-Bensemra Investigation of polyethylene pipeline behavior after 30 Years of use in gas distribution network J. Mater. Eng. Perform., 29 (10) (2020), pp. 6652-6660

[4] A. Bianchini, et al. Natural gas distribution system: a statistical analysis of accidents data

Int. J. Pres. Ves. Pip., 168 (2018), pp. 24-38

[5] M. Doaei, M.S. Tavallali Intelligent screening of electrofusion-polyethylene joints based on a thermal NDT method Infrared Phys. Technol., 90 (2018), pp. 1-7

[6] M. Doaei, M.S. Tavallali, H. Nejati Fault classification in electrofusion polyethylene joints by combined machine learning, thermal pulsing and IR thermography methods–A comparative study Infrared Phys. Technol., 96 (2019), pp. 262-266

[7] M. Sahlabadi, N. Soltani Experimental and numerical investigations of mixed-mode ductile fracture in high-density polyethyleneArch. Appl. Mech., 88 (6) (2018), pp. 933-942

[8] Y. Zhang, J. Shi, J. Zheng Study of mode I-II mixed crack propagation in electrofusion joint of polyethylene pipe Pressure Vessels and Piping Conference, American Society of Mechanical Engineers (2018)

[9] C. O'Connor, G.N. Denton Polyethylene pipeline systems: avoiding the pitfalls of fusion welding Proceedings of the 7th Pipeline Technology Conference (2012) Hannover, Germany

[10] S.S. Say, A. Akgüngör Welding defects and their reasons observed in electrofusion welding of polyethylene pipes 24th World Gas Conference, WGC Argentina (2009)

[11] D. Sarambale, D. Shinde Electro-Fusion joint failure polyethylene pipes analysis and its simulation using finite element analysis Int. J. Mech. Product. Eng., 5 (12) (2017), pp. 51-55

[12] P. Tayefi, S. Beck, R. Tomlinson The fatigue performance of electrofusion tapping tees subject to contamination Int. J. Pres. Ves. Pip., 171 (2019), pp. 271-277

[13] G. Marshall, D. Hepburn, N. Netherwood Improvements in electrofusion welding in the US water industry Proc. Plastic. Pipes, IX (1995), pp. 153-161

[14] M.J. Troughton Handbook of Plastics Joining: a Practical Guide William Andrew (2008)

[15] J. Bowman A review of the electrofusion joining process for polyethylene pipe systems Polym. Eng. Sci., 37 (4) (1997), pp. 674-691

[16] R. Tikhonov, et al. Calculation of the thermal and stress-strain states in electrofusion welding of polyethylene pipes in thermoelastic statement AIP Conference Proceedings., AIP Publishing LLC (2018)

[17] N. Starostin, O. Ammosova Calculation of the technological parameters of electrofusion welding of polyethylene pipes at low temperatures AIP Conference Proceedings., AIP Publishing LLC (2017)

[18] I. Ramadan, M. Tanase Experimental study regarding the influence of welding parameters on the mechanical behavior of high density polyethylene pipes Mater. Plast., 57 (4) (2020), pp. 209-215

[19] A. Najafigharehtapeh, R. Kacar An effect of environment temperature and pre-heat treatment on the electrofusion welding of polyethylene natural gas pipes J. Faculty Eng. Architect. Gazi Univ., 33 (2) (2018), pp. 371-380

[20] A. Tutunchi, et al. Risk assessment of an urban natural gas polyethylene piping system J. Pipeline Syst. Eng. Pract., 11 (2) (2020), p. 6019005

[21] M.P. Gierulski, R. Tomlinson, M. Troughton Electrofusion welding and reinforced thermoplastic pipes–A review J. Reinforc. Plast. Compos. (2021) 07316844211051207

[22] Z. Ge, et al. A comprehensive review on failure analysis of electrofusion joint for plastic pipes Pressure Vessels and Piping Conference, American Society of Mechanical Engineers (2021)

[23] J.K. Maupin Plastic pipe failure analysis 2008 7th International Pipeline Conference (2008), pp. 399-407

[24] J. Mora-Rodríguez, et al. An overview of leaks and intrusion for different pipe materials and failures Urban Water J., 11 (1) (2014), pp. 1-10

[25] A.M.S. Clair, S. Sinha Development of a standard data structure for predicting the remaining physical life and consequence of failure of water pipes J. Perform. Constr. Facil., 28 (1) (2014), pp. 191-203

[26] R.K. Krishnaswamy Analysis of ductile and brittle failures from creep rupture testing of high-density polyethylene (HDPE) pipes Polymer, 46 (25) (2005), pp. 11664-11672

[27] H. Li, et al. Ductile fracture: experiments and computations Int. J. Plast., 27 (2) (2011), pp. 147-180

[28] K. Osouli-Bostanabad, A. Tutunchi, M. Eskandarzade The influence of pre-bond surface treatment over the reliability of steel epoxy/glass composites bonded joints Int. J. Adhesion Adhes., 75 (2017), pp. 145-154

[29] H.B.H. Hamouda, et al. Creep damage mechanisms in polyethylene gas pipes Polymer, 42 (12) (2001), pp. 5425-5437

[30] N. Merah, et al. Effect of temperature on tensile properties of HDPE pipe material Plastics, Rubber Compos., 35 (5) (2006), pp. 226-230

[31] K. Leskovics, M. Kollár, P. Bárczy A study of structure and mechanical properties of welded joints in polyethylene pipes Mater. Sci. Eng., A, 419 (1) (2006), pp. 138-143

Figure captions

Fig. 1. Flowchart of working steps of current study.

Fig. 2. Flowchart of the FMEA process.

Fig. 3. Risk matrix to combine COFs and POFs.

Fig. 4. Apparatus to produce man-made defects in welding zones. (a) Schematic of a stencil for accurate production of lipid pollution and moisture type defects; (b) Apparatus used for the production of improper scraping with dimensions of 35 mm × 15 mm

Fig. 5. (a) The lipid type pollutant on a pipe surface before the welding process; (b) Example of improper scraping on a welding surface.

Fig. 6. Final experimental setup for electrofusion welding.

Fig. 7. CT-scans of electrofusion joints (A) without defect, (B) with improper scrap, (C) with trapped humidity, and (D) with a lipid type pollution.

Fig. 8. Shows crushing de-cohesion test on electrofusion joints. Crushing tests showed no considerable differences between appropriately welded and defective joints.

Fig. 9. Optical Macroscopy (×50) presentation of fractured surface of the electrofusion welding after strip-bend test containing, (a) improper scraping, (b) humidity, (c) lipid type defects.

Fig. 10. The microscopic presentation of the fractured surfaces in defective areas of the electrofusion joints after strip-bend tests, (a) Improper scraping (b) Humidity, (c) lipid type defects.

Fig. 11. SEM observation of fractured surfaces with magnification of 100X, (a) Lipid type defect, (b) Humidity type defect.

Fig.1

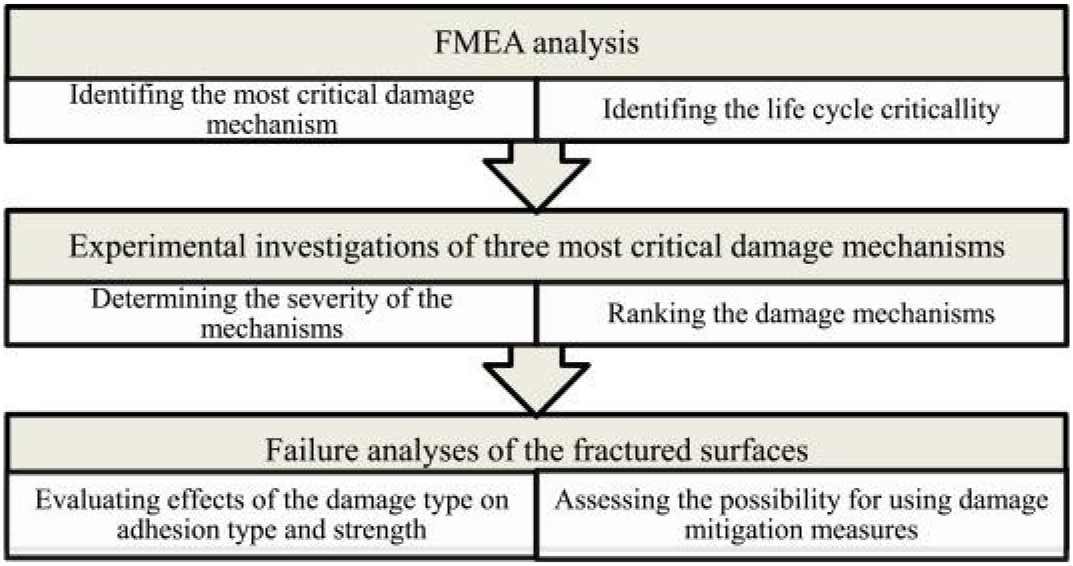
FMEA analysis
Identifing the most critical damage mechanism
Identifing the life cycle criticallity
Experimental investigations of three most critical damage mechanisms
Determining the severity of the mechanisms
Ranking the damage mechanisms
Failure analyses of the fractured surfaces
Evaluating effects of the damage type on adhesion type and strength
Assessing the possibility for using damage mitigation measures

Fig. 2

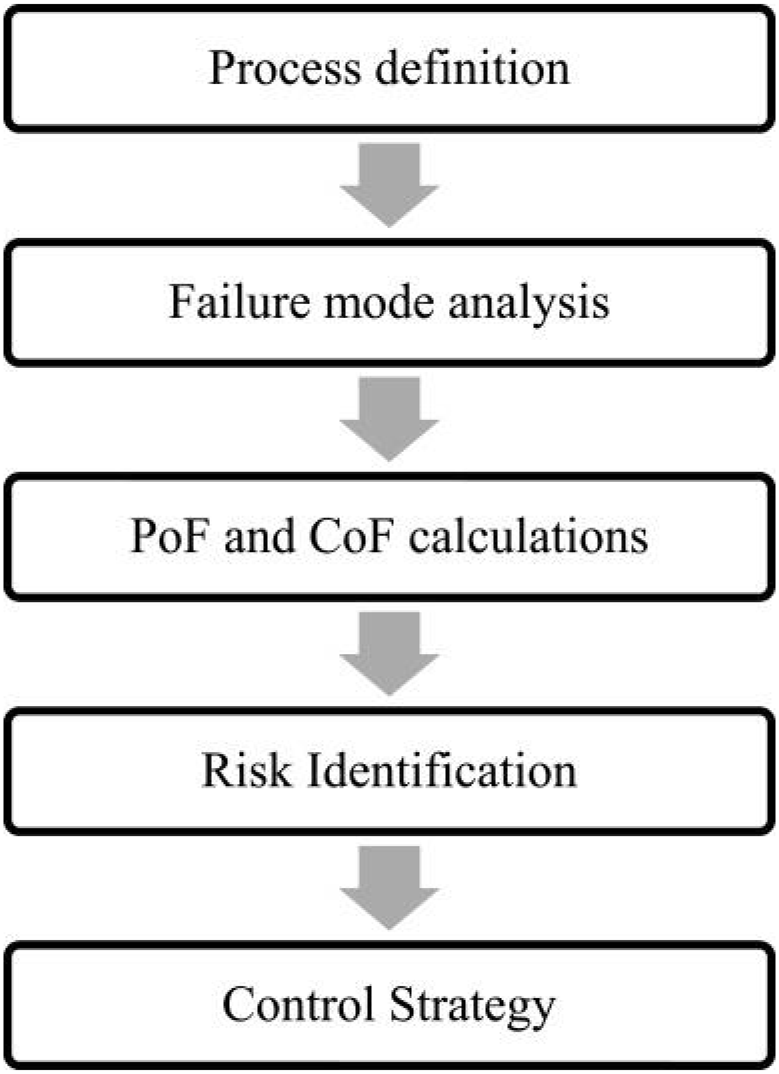
Process definition
Failure mode analysis
PoF and CoF calculations
Risk Identification
Control Strategy

Fig. 3

| | | | | | |
|---|---|---|---|---|---|
| 5 | MH | MH | MH | H | H |
| 4 | M | M | MH | MH | H |
| 3 | L | L | M | MH | H |
| 2 | L | L | M | M | MH |
| 1 | L | L | M | M | MH |
| | A | B | C | D | E |

Fig. 4

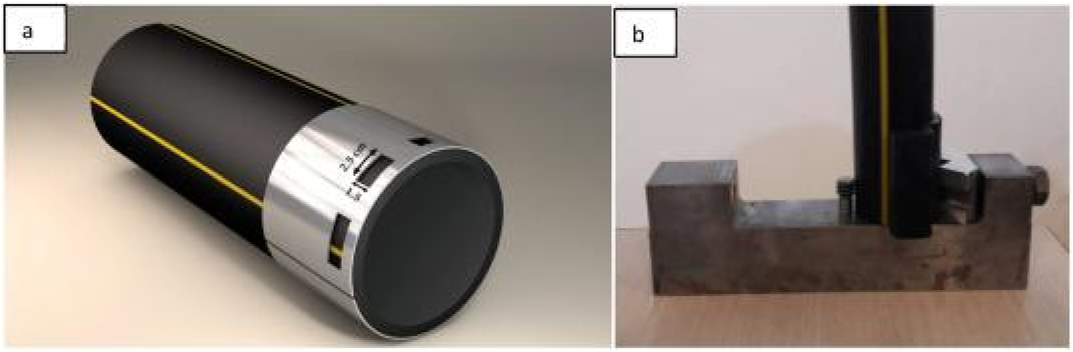

Fig. 5

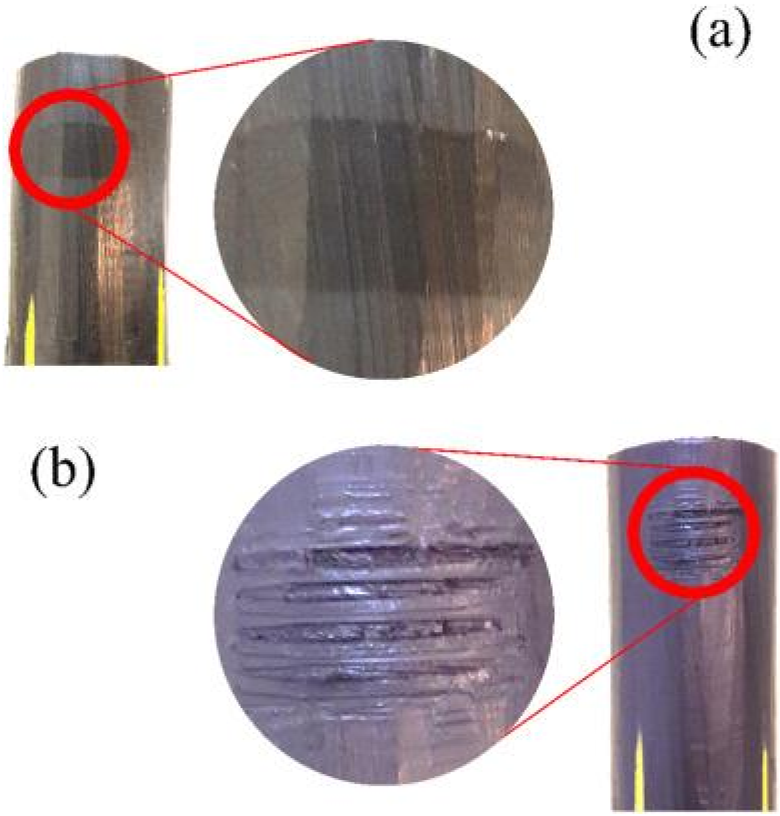

Fig. 6

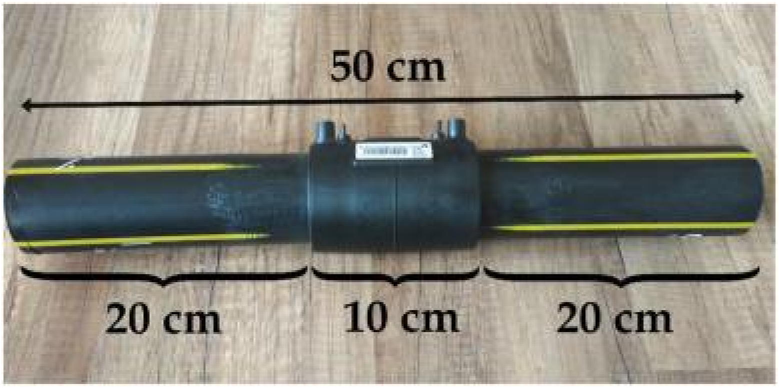

Fig. 7

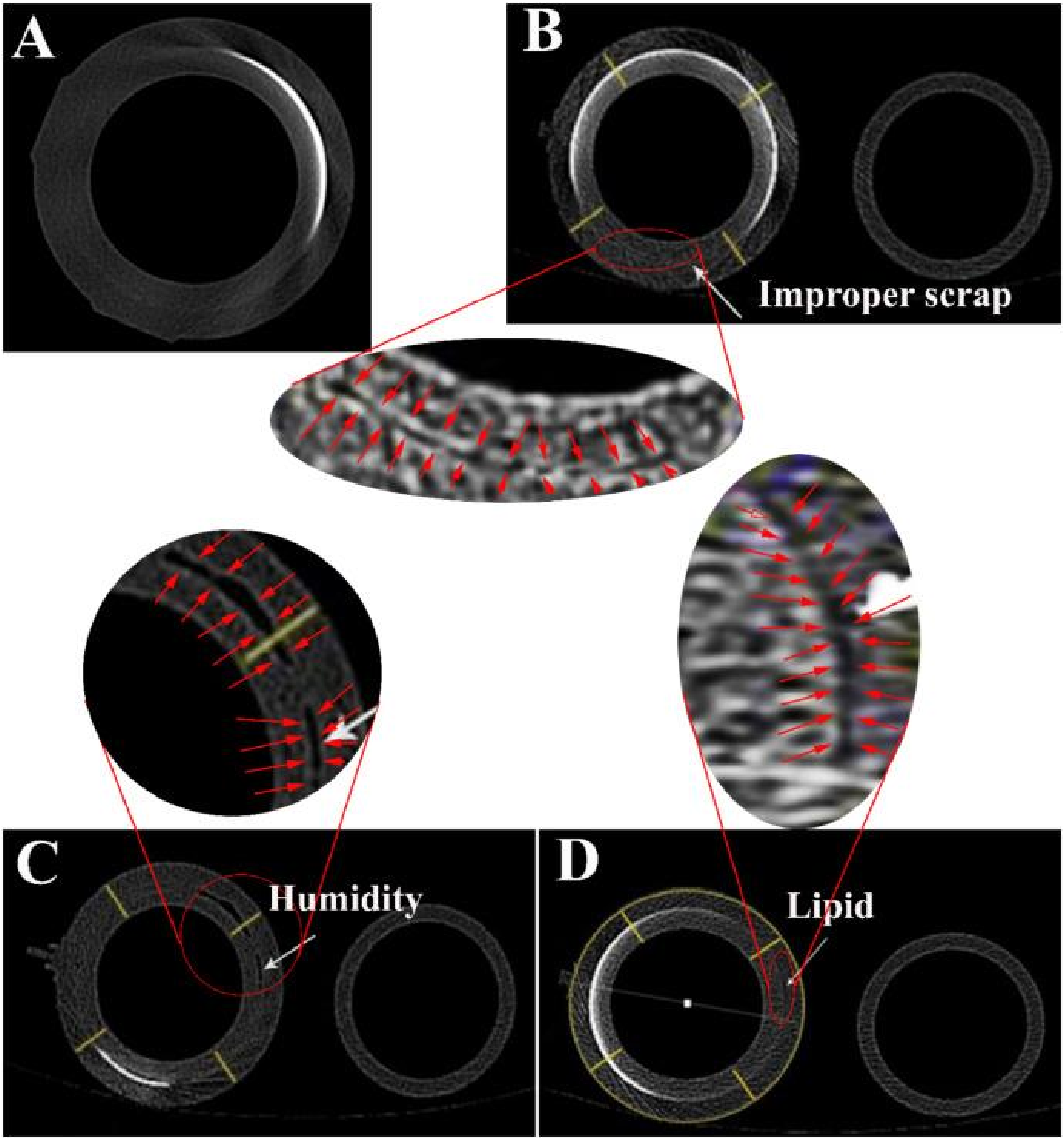

Fig. 8

Fig. 9

Fig. 10

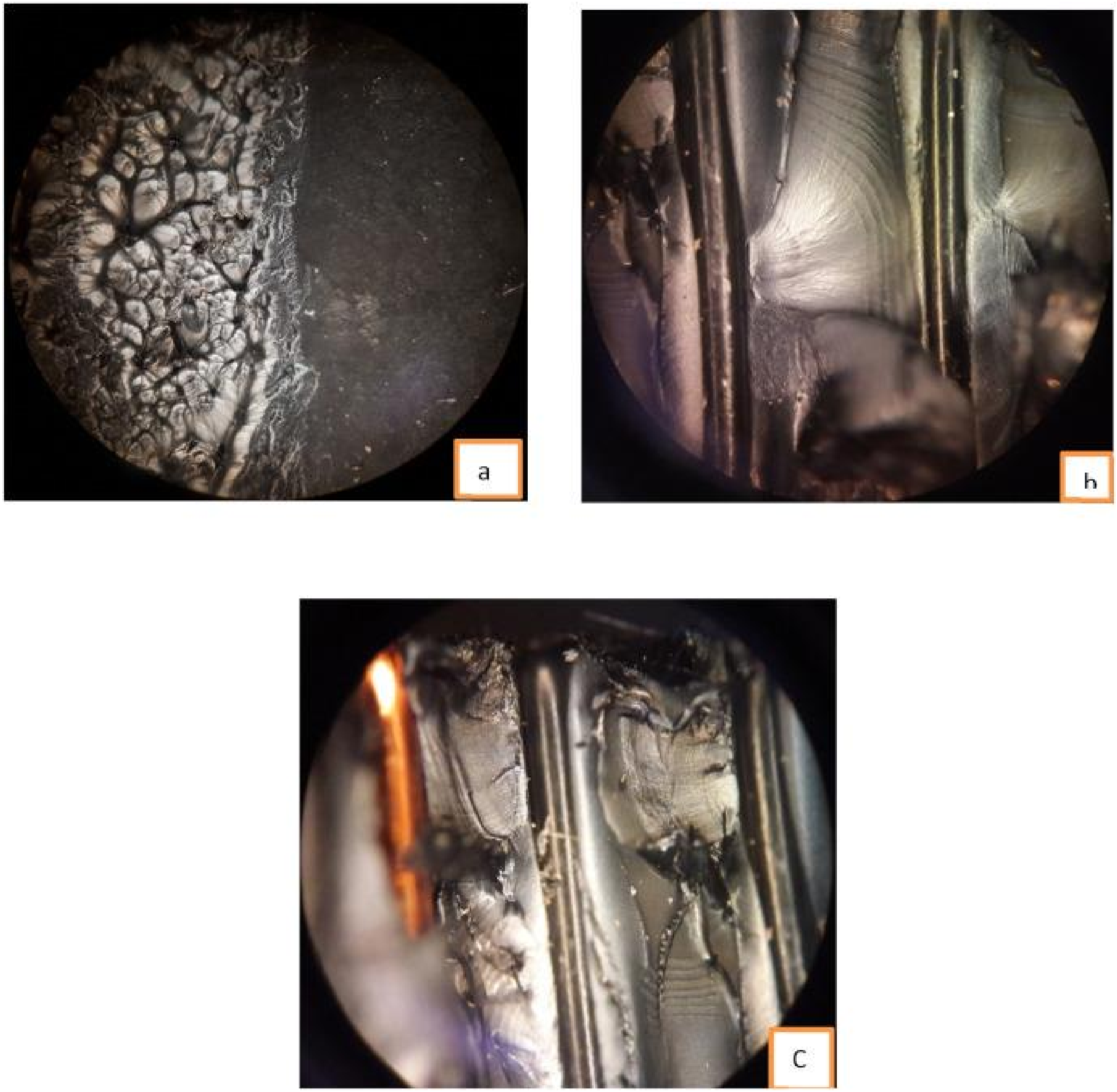

Fig. 11